Photochemical Formation and Thermal Rearrangements of $Mn_2(CO)_9PR_3$ and $Mn_2(CO)_8(PR_3)_2$ Isomers

Hai-Tao Zhang and Theodore L. Brown*

Contribution from the School of Chemical Sciences and Beckman Institute for Advanced Science and Technology, University of Illinois, Urbana-Champaign, Urbana, Illinois 61801.
Received May 26, 1992

Abstract: Solutions in 3-methylpentane of $Mn_2(CO)_{10}$ and PR_3 (R = alkyl) or of $Mn_2(CO)_8(PR_3)_2$ have been flash-photolyzed at various temperatures from 90 to 297 K, using a xenon flash lamp, and the photolysis products have been observed using IR or UV-visible spectroscopy. Use of flash photolysis rather than continuous photolysis and maintenance of low temperatures permit the observation of many intermediates not previously observed. The primary photoprocesses are CO loss and Mn-Mn bond homolysis. At 90 K in 3-methylpentane glass, only the product of CO loss is observed. A solvent-coordinated species, $Mn_2(CO)_9(S)$ (S = solvent), is formed initially, as the result of multiple-flash photolysis of solution samples containing $Mn_2(CO)_{10}$, and is replaced by the semibridging form, $Mn_2(CO)_8(\mu\text{-}\eta^1,\eta^2\text{-CO})$. At temperatures above about 145 K, where the medium is fluid, diffusive separation of $Mn(CO)_5$ or $Mn(CO)_4PR_3$ radicals occurs. The unsubstituted radicals undergo rapid substitution; $Mn(CO)_4PR_3$ radicals recombine, forming $Mn_2(CO)_8(PR_3)_2$. The IR spectra reveal that the immediate product of recombination for $PR_3 = P(n\text{-Bu})_3$ and $P(i\text{-Bu})_3$ is the bis-equatorial isomer, *e,e*-$Mn_2(CO)_8(PR_3)_2$. This species isomerizes directly to the thermodynamic product, *a,a*-$Mn_2(CO)_8(PR_3)_2$, without the intermediacy of the a,e-isomer. The semibridging species formed initially following CO loss from *a,a*-$Mn_2(CO)_8(PR_3)_2$ appears from the IR spectra to have the phosphines in axial positions. In the temperature range of 173 K there is a slow isomerization to form two distinct species, assigned as a,e-isomers. Recombination with CO leads to *a,e*-$Mn_2(CO)_8(PR_3)_2$, which then isomerizes to the a,a-isomer. Comparisons of the low temperature UV-visible spectra with the IR spectra at low temperature, as well as the application of conventional laser pulse transient spectroscopy, permit assignment of absorption bands to intermediate species: $Mn_2(CO)_9$* (* denotes semibridge), 500 nm; *a,a*-$Mn_2(CO)_7[P(n\text{-Bu})_3]_2$*, 530 nm; *a,e*-$Mn_2(CO)_8[P(n\text{-Bu})_3]_2$, 420 nm; *e,e*-$Mn_2(CO)_8[P(n\text{-Bu})_3]_2$, 440 nm; *e*-$Mn_2(CO)_9P(i\text{-Bu})_3$, 420 nm; *a*-$Mn_2(CO)_9P(i\text{-Bu})_3$, 414 nm. Using transient absorption techniques, with either pulsed laser flash (308 nm) or xenon flash lamp photolysis, the following rate constants were measured at 297 K: *e*-$Mn_2(CO)_9P(n\text{-Bu})_3 \rightarrow$ *a*-$Mn_2(CO)_9P(n\text{-Bu})_3$, 12 s^{-1}; *e,e*-$Mn_2(CO)_8[P(n\text{-Bu})_3]_2 \rightarrow$ *a,a*-$Mn_2(CO)_8[P(n\text{-Bu})_3]_2$, 1.5×10^3 s^{-1}; $Mn_2(CO)_7[P(n\text{-Bu})_3]_2$* + CO $\rightarrow$ *a,e*-$Mn_2(CO)_8[P(n\text{-Bu})_3]_2$, 5.7×10^3 M^{-1} s^{-1}; *a,e*-$Mn_2(CO)_8[P(n\text{-Bu})_3]_2 \rightarrow$ *a,a*-$Mn_2(CO)_8[P(n\text{-Bu})_3]_2$, 6 s^{-1}. The isomerizations appear to be intramolecular in character. The surprisingly high rate constant for e,e $\rightarrow$ a,a interconversion and the absence of an intermediate a,e-isomer are accounted for in terms of pairwise CO bridge formation as the pathway for exchange. Bulky ligands such as $P(C_6H_{11})_3$ or $P(i\text{-Pr})_3$ form only *a,e*-$Mn_2(CO)_8(PR_3)_2$ on recombination of radicals; the a,e-isomer converts to the stable a,a-form at a rate slower than that of the $P(n\text{-Bu})_3$ analogue. For PMe_3, *e,e*-$Mn_2(CO)_8(PMe_3)_2$ is the stable form; it is re-formed on recombination of $Mn(CO)_4PMe_3$ radicals. However, recombination of CO with the CO-loss product yields significant quantities of *a,e*-$Mn_2(CO)_8(PMe_3)_2$ as initial product.

The substitution reactions of group 7 dinuclear carbonyls have been the subjects of several reports.[1] Both thermal and photochemical pathways for substitution are known. The thermal reactions of both $Mn_2(CO)_{10}$ and $Re_2(CO)_{10}$ proceed via dissociative CO loss.[1e,2] The photochemical processes have been extensively studied.[3] Substitution proceeds via both CO loss and metal-metal bond homolysis, with relative quantum yields that vary with irradiating wavelength.[4]

Because the $Mn(CO)_5$ radicals produced in photochemical Mn-Mn bond homolysis are highly labile toward substitution,[5] under typical conditions the disubstituted dimer, $Mn_2(CO)_8L_2$, is the dominant product of reaction via this pathway.[3] $Mn(CO)_5$ radicals undergo recombination with second-order rate constants of about 1×10^9 M^{-1} s^{-1}, near the diffusion limit. The rate constants for recombination of substituted radicals are smaller, decreasing as the size of the ligand increases.[3g]

On the other hand, CO loss leads to formation of a linear semibridging $Mn_2(CO)_9$ intermediate,[4b,6] which reacts with ligand to form the monosubstituted product, $Mn_2(CO)_9L$.[3d,4b,7] The transient spectra of the CO-loss species, $Mn_2(CO)_7L_2$, of a series of disubstituted dimers and the rates of reaction with CO have been observed.[3d]

In general, photochemical reaction of $Mn_2(CO)_{10}$ with a monodentate phosphorus ligand leads to both mono- and disubstituted products. Except for the smallest ligands (e.g., CH_3CN, PMe_3), the substituents are found in the axial positions (a,a-isomer). There have been few reports of dimers of the form $Mn_2(CO)_7L_3$, where L is monodentate.[3c,8] In three cases of the type $Mn_2(CO)_6(L\text{-}L)_2$, where L-L is a bidentate ligand, the ligands are bridging between the two metals.[9] Compounds of the form $Mn_2(CO)_6L_4$, where L is monodentate, containing a stable Mn-

* Author to whom correspondence should be addressed at the School of Chemical Sciences.

(1) (a) Geoffroy, G. L.; Wrighton, M. S. *Organometallic Photochemistry*; Academic: New York, 1978. (b) Meyer, T. J.; Caspar, J. V. *Chem. Rev.* **1985**, *85*, 187. (c) Yasufuku, K.; Noda, H.; Iwai, J.; Ohtani, H.; Hoshino, M.; Kobayashi, T. *Organometallics* **1985**, *4*, 2174. (d) Firth, S.; Klotzbücher, W. E.; Poliakoff, M.; Turner, J. J. *Inorg. Chem.* **1987**, *26*, 3370. (e) Basolo, F. *Polyhedron* **1990**, *9*, 1503. (f) Coville, N. J. In *Organometallic Radical Processes*; Trogler, W. C., Ed.; Elsevier: Amsterdam, 1990; p 108.

(2) (a) Basolo, F.; Wawersik, H. *Inorg. Chim. Acta* **1969**, *3*, 113. (b) Sonnenberger, D.; Atwood, J. D. *J. Am. Chem. Soc.* **1980**, *102*, 3484. (c) Schmidt, S. P.; Trogler, W. C.; Basolo, F. *Inorg. Chem.* **1982**, *21*, 1698. (d) Muetterties, E. L.; Burch, R. R.; Stolzenberg, A. M. *Annu. Rev. Phys. Chem.* **1982**, *33*, 89. (e) Stolzenberg, A. M.; Muetterties, E. L. *J. Am. Chem. Soc.* **1983**, *105*, 822. (f) Coville, N. J.; Stolzenberg, A. M.; Muetterties, E. L. *J. Am. Chem. Soc.* **1983**, *105*, 2499. (g) Schmidt, S. P.; Basolo, F.; Jensen, C. M.; Trogler, W. C. *J. Am. Chem. Soc.* **1986**, *108*, 1894.

(3) (a) Wrighton, M. S.; Ginley, D. S. *J. Am. Chem. Soc.* **1975**, *97*, 2065. (b) Hughey, J. L.; Anderson, C. P.; Meyer, T. J. *J. Organomet. Chem.* **1977**, *125*, C49. (c) Kidd, D. R.; Brown, T. L. *J. Am. Chem. Soc.* **1978**, *100*, 4095. (d) Herrick, R. S.; Brown, T. L. *Inorg. Chem.* **1984**, *23*, 4550. (e) McCullen, S. B.; Brown, T. L. *Inorg. Chem.* **1981**, *20*, 3528. (f) Nubel, P. O.; Brown, T. L. *J. Am. Chem. Soc.* **1984**, *106*, 644. (g) Walker, H. W.; Herrick, R.; Olsen, R. J.; Brown, T. L. *Inorg. Chem.* **1984**, *23*, 3748.

(4) (a) Kobayashi, T.; Ohtani, H.; Noda, H.; Teratani, S.; Yamazaki, H.; Yasufuku, K. *Organometallics* **1986**, *5*, 110. (b) Seder, T. A.; Church, S. P.; Weitz, E. *J. Am. Chem. Soc.* **1986**, *108*, 7581.

(5) (a) Poë, A. *Transition Met. Chem.* **1982**, *7*, 65. (b) Herrinton, T. R.; Brown, T. L. *J. Am. Chem. Soc.* **1985**, *107*, 5700.

(6) (a) Hepp, A. F.; Wrighton, M. S. *J. Am. Chem. Soc.* **1983**, *105*, 5934. (b) Church, S. P.; Hermann, H.; Grevels, F.-W.; Schaffner, K. *J. Chem. Soc., Chem. Commun.* **1984**, 785. (c) Dunkin, I. R.; Härter, P.; Shields, C. *J. Am. Chem. Soc.* **1984**, *106*, 7248.

(7) (a) Yesaka, H.; Kobayashi, T.; Yasufuku, K.; Nagakura, S. *J. Am. Chem. Soc.* **1983**, *105*, 6249. (b) Kobayashi, T.; Yasufuku, K.; Iwai, J.; Yesaka, H.; Hoda, H.; Ohtani, H. *Coord. Chem. Rev.* **1985**, *64*, 1. (c) Sullivan, R. J.; Brown, T. L. *J. Am. Chem. Soc.* **1991**, *113*, 9155. (d) Sullivan, R. J.; Brown, T. L. *J. Am. Chem. Soc.* **1991**, *113*, 9162.

0002-7863/93/1515-107$04.00/0

Mn bond, are rare. The steric requirements of the ligands so weaken the metal–metal bond that persistent $Mn(CO)_3L_2$ radicals are observed instead.[10]

The importance of the CO-loss pathway in the photochemical reactions of $Mn_2(CO)_{10}$ and related dinuclear compounds was not fully appreciated in earlier work. The work reported here is an outgrowth of a program to more fully characterize the pathways for photochemical substitution in dinuclear manganese carbonyls in light of recent studies of the photochemical reactions of $Mn_2(CO)_8L_2$ compounds with $HSnBu_3$.[7c,d] In that work it became evident that reaction occurs only via the CO-loss pathway. Further, the kinetics of the reactions reflected a stabilization of the CO-loss intermediate as a result of semibridge formation. We speculated that it might be possible to observe the effects of semibridge formation on the reactions of the $Mn_2(CO)_7L_2$ intermediates with other nucleophiles, such as phosphines.

In the attempt to study these reactions in detail, we discovered that the processes involving both the CO-loss and radical pathways are more complex than previously thought. The initial, kinetic products in both cases are not the thermodynamic products. We report here on the photochemically-generated intermediates formed upon irradiation of solutions of $Mn_2(CO)_8L_2$ compounds or $Mn_2(CO)_{10}$ in the presence of phosphorus ligands and the subsequent thermal isomerization processes. We have employed flash photolysis at low temperatures with low-temperature IR detection to prepare and identify various unstable intermediates and to follow the further transformation of these unstable initial products to the thermodynamic products. The dynamic processes are observed as well in room-temperature flash photolysis experiments with UV–visible detection.

Experimental Section

Solvents. A. **Hexane** (Burdich and Jackson Laboratories, Inc.) was purified following a literature method[7c] with a slight modification that the distilled solvent was stored over 4-Å molecular sieves inside the glovebox.

B. **3-Methylpentane** (Aldrich) was distilled over CaH_2 and collected under Ar atmosphere. The distillate was further degassed via three to four freeze–pump–thaw cycles before storage over the molecular sieves in a glovebox.

Reagents. A. **Manganese carbonyl** ($Mn_2(CO)_{10}$, Pressure Chemical Co.) was purified by sublimation and stored in a refrigerator before use.

B. **Disubstituted manganese carbonyl compounds** $Mn_2(CO)_8L_2$ (L = $P(n\text{-}Bu)_3$, $P(i\text{-}Bu)_3$, PMe_3, $P(i\text{-}Pr)_3$, **and** PCy_3) were prepared and purified by Dr. Richard J. Sullivan, as reported previously.[7c]

C. $P(n\text{-}Bu)_3$ **and** $P(i\text{-}Bu)_3$ were purified by distillation over CaH_2 under vacuum. After further degassing through several freeze–pump–thaw cycles, they were stored under an Ar atmosphere.

D. **Carbon monoxide** (Matheson Gas Products, Inc., Matheson purity grade, 99.99%) was first purged of $Fe(CO)_5$ by being passed through a copper tube filled with activated charcoal at about 180 °C and then a second tube in a dry ice/ethanol bath. It was further purified by being passed through an oxygen trap (American Scientific) before introduction into the solution sample.

Low-Temperature IR Spectroscopy. The experiments were conducted with a Specac Variable Temperature Cell P/N 21500 in a Perkin-Elmer 1710 FTIR spectrophotometer. The cell assembly consists of a gas-tight cell, a cell holder and refrigerant chamber, a vacuum jacket, and an external temperature controller. Depending on the desired temperature, liquid N_2 or a dry ice/acetone mixture was used as the refrigerant. In general, liquid N_2 was used when the required temperature was below 210 K, and the dry ice/acetone mixture for higher temperatures. Due to the existence of temperature gradients, the actual temperature of the sample could be lower than the recorded temperature when liquid N_2 is used as the refrigerant.

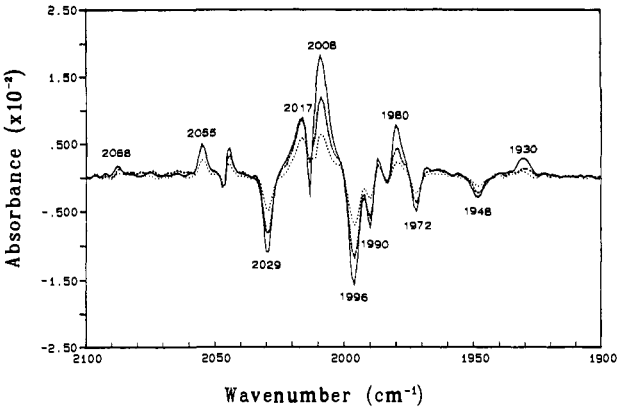

Figure 1. Difference IR spectra of a 3-methylpentane solution sample containing 4.9×10^{-4} M $Mn_2(CO)_{10}$ and 1.0×10^{-2} M $P(n\text{-}Bu)_3$ subjected to multiple-flash photolysis at 90 K (with the spectrum taken at 1 min after the flashes as the reference). The three spectra represent respectively the differences between the spectra collected at 10 (···), 20 (---), and 40 min (—) after the photolysis and the spectrum at 1 min. Positive absorbances correspond to increasing IR absorbance in the IR spectra in the time interval involved; negative absorbances correspond to decreases in absorbances in the same time intervals. Not shown here is the peak at 1760 cm^{-1}, which increases continuously over 30 min following the flashes.

Typically, a sample solution was loaded into the IR cell inside an Ar-filled glovebox. After the cell was installed in the holder, the system was connected to a vacuum pump. The desired temperature was reached and held constant with a suitable refrigerant and use of the controller. Photolysis was effected in the Xe flash apparatus with either single or multiple flashes. The assembly was then immediately moved to the FTIR spectrophotometer, and spectra were recorded.

Low-Temperature UV–Visible Spectroscopy. With the same low-temperature IR cell assembly and the same sample manipulation and photolysis procedure, UV–visible spectra of a sample at a controlled temperature were obtained with an HP 8452A diode array spectrophotometer.

Laser and Xe Lamp Flash Photolyses. Both laser and xenon flash lamp transient techniques were employed to study the decay of various intermediates. Pulsed laser flashes were obtained with a XeCl excimer laser, yielding 308-nm pulses of about 30-ns width. The detailed operations of both instruments were similar to those described elsewhere.[7d,11] All solution samples were prepared inside an Ar-filled glovebox. The solution samples saturated with CO were manipulated according to literature methods.[12]

Results

Low-Temperature Flash Photolysis of $Mn_2(CO)_{10}$ Solutions Containing Excess Phosphorus Ligands. Hydrocarbon (3-methylpentane) solutions of $Mn_2(CO)_{10}$ and excess $P(n\text{-}Bu)_3$ in an IR cell within a low-temperature probe were subjected to xenon flash lamp irradiation at various temperatures. Following irradiation the cell was quickly taken to an FTIR spectrometer and the IR spectra were recorded from time to time while low-temperature conditions were maintained. For solutions containing 4.9×10^{-4} M $Mn_2(CO)_{10}$ and 1.0×10^{-2} M $P(n\text{-}Bu)_3$, after multiple flashes at 90 K, the difference IR spectra indicate formation of the linear semibridging species, $Mn_2(CO)_8(\mu\text{-}\eta^1,\eta^2\text{-}CO)$, which we denote as $Mn_2(CO)_9$*; bands at 2055, 2017, 1987, 1963, and 1760 cm^{-1}, previously assigned to the semibridged species,[4b,6] are seen. The concentration of this species shows a small apparent increase in the first 30 min following irradiation and then decreases slowly at 90 K. Additional bands apparent after photolysis can be classified into two groups. One group mainly consists of absorbance peaks at 2029, 1996, 1990, 1972, and 1948 cm^{-1}. The intensities of these bands decrease continuously over about 30 min, during which time the bands due to the semibridged species grow to their maximum, most obviously at 2055, 2017, and 1760 cm^{-1}

(8) (a) Mathey, F. *J. Organomet. Chem.* **1975**, *93*, 377. (b) Kasanally, A. S.; Nyholm, R. S.; Parker, D. J.; Stiddard, M. H. B.; Hodder, O. J. R.; Powell, H. M. *Chem. Ind. (London)* **1965**, 2097.

(9) (a) Nyholm, R. S.; Rao, D. V. *Proc. Chem. Soc., London* **1959**, 130. (b) Reimann, R. H.; Singleton, E. *J. Organomet. Chem.* **1972**, *38*, 113. (c) Colton, R.; Commons, G. J. *Aust. J. Chem.* **1975**, *28*, 1673. (d) Commons, G. J.; Hoskins, B. F. *Aust. J. Chem.* **1975**, *28*, 1663. (e) Colton, R.; Commons, G. J.; Hoskins, B. F. *J. Chem. Soc., Chem. Commun.* **1975**, 363. (f) Caulton, K. G.; Adair, P. *J. Organomet. Chem.* **1976**, *114*, C11.

(10) (a) Kidd, D. R.; Cheng, C. P.; Brown, T. L. *J. Am. Chem. Soc.* **1978**, *100*, 4103. (b) McCullen, S. B.; Brown, T. L. *J. Am. Chem. Soc.* **1982**, *104*, 7496.

(11) Herrick, R. S.; Herrinton, T. R.; Walker, H. W.; Brown, T. L. *Organometallics* **1985**, *4*, 42.

(12) Zhang, S.; Dobson, G. R.; Brown, T. L. *J. Am. Chem. Soc.* **1991**, *113*, 6908.

Table I. IR Absorption Band Frequencies of Intermediates

compounds[a]	IR wave number (cm^{-1})	ref
$Mn_2(CO)_9$*	2055 (s), 2017 (s), 1987 (s), 1963 (w), 1760 (w)	6
a,a-$Mn_2(CO)_7[P(n\text{-}Bu)_3]_2$*	2035 (w), 1976 (w), 1944 (s), 1902 (w), 1701 (w)	*c*
a-$Mn_2(CO)_7(PCy_3)_2$*	2031 (m), 1980 (m), 1942 (s), 1916 (w), 1898 (w), 1882 (w), 1699 (m)	*c*
a-$Mn_2(CO)_7[P(i\text{-}Pr)_3]_2$*	2033 (m), 1980 (m), 1945 (s), 1902 (w), 1701 (m)	*c*
a,e-$Mn_2(CO)_7[P(n\text{-}Bu)_3]_2$*	2029 (w), 1981 (w), 1952 (s), 1915 (m), 1889 (m), 1715 (s), 1687 (s)	*c*
e-$Mn_2(CO)_7(PMe_3)_2$*	2031 (w), 1986 (m), 1955 (s), 1929 (m), 1887 (m), 1717 (w), 1692 (?vw)	*c*
$Mn_2(CO)_9(S)$	2029 (s), 1996 (s), 1990 (m), 1972 (m), 1948 (m)	*c*
$Mn_2(CO)_9(CH_3CN)$	2092 (w), 2033 (s), 2002 (s), 1990 (s), 1966 (s), 1949 (m)	13
e-$Mn_2(CO)_9P(n\text{-}Bu)_3$	2088 (m), 2006 (s), 1990 (s), 1980 (s), 1970 (m), 1955 (w), 1939 (w), 1930 (m)	*c*
e-$Mn_2(CO)_9py$	2089 (w), 2016 (s), 2005 (m), 1980–83 (s), 1962 (m), 1943 (m)	13
e-$Mn_2(CO)_9pic$	2084 (w), 2013 (s), 2005 (m), 1983 (s), 1978 (s), 1961 (m), 1942 (m)	13
a-$Mn_2(CO)_9P(n\text{-}Bu)_3$	2090 (w), 2008 (m), 1990 (s), 1970 (w), 1941 (vw), 1933 (m)	*c*
a-$Mn_2(CO)_9PPh_3$	2091 (w), 2011 (w), 1998 (s), 1976 (w), 1941 (m)	13
e,e-$Mn_2(CO)_8[P(n\text{-}Bu)_3]_2$	1977 (s), 1955 (s), 1910 (s)	
e,e-$Mn_2(CO)_8(AsMe_3)_2$	2055 (m), 1986 (s), 1959 (s), 1918 (s)	17
e,e-$Mn_2(CO)_8(PMe_2Ph)_2$	2055 (w), 1989 (s), 1956 (s), 1914 (s)	17
e,e-$Mn_2(CO)_8(AsEt_3)_2$	2055 (w), 1980 (s), 1952 (s), 1927 (w), 1915 (m)	17
e,e-$Mn_2(CO)_8(PMe_3)_2$	2053 (w), 1983 (m), 1956 (s), 1918 (m)	3d
e,e-$Mn_2(CO)_8[P(n\text{-}Bu)_3]_2$	1977 (s), 1955 (s), 1910 (s)	*c*
a,e-$Mn_2(CO)_8[P(n\text{-}Bu)_3]_2$	2050 (m), 1977 (s), 1966 (s), 1957 (s), 1920 (s), 1914 (s), 1904 (m), 1891 (w)	*c*
a,e-$Mn_2(CO)_8(PCy_3)_2$	2055 (m), 1976 (w), 1957 (s), 1923 (w), 1912 (w)	*c*
a,e-$Mn_2(CO)_8[P(i\text{-}Pr)_3]_2$	2057 (s), 1978 (s), 1959 (s), 1930 (w)	*c*
a,e-$Mn_2(CO)_8(PMe_3)_2$[b]	2053 (w), 2007 (w), 1961 (m), 1942 (s), 1917 (s), 1905 (m), 1863 (w)	*c*
a,e-$Re_2(CO)_8(PPh_3)_2$	2069 (mw), 2012 (m), 1964 (vs, br), 1934 (m), 1921 (m)	3f
a,e-$Re_2(CO)_8[P(n\text{-}Bu)_3]_2$	2068 (mw), 2006 (m), 1971 (s), 1928 (s), 1917 (s)	3f

[a] An asterisk denotes the semibridging form of the CO-loss molecule. [b] Some peaks are broad; they may contain contributions from other isomeric components, e.g., the a,a-isomer. [c] Present work.

(Figure 1). The other bands, mostly at 2088, 2008, 1980, and 1930 cm^{-1}, with continuously increasing intensities, as shown in this figure, originate in other species, probably P(*n*-Bu)$_3$-substituted compounds, which are discussed in detail in the next few paragraphs. The pattern of IR bands of the decaying transient species is very similar to that expected for a monosubstituted derivative. For example, the pattern of IR bands ascribed to $Mn_2(CO)_9(CH_3CN)$ is shown in Table I for comparison.[13] Except for the absence of the highest frequency band, which in any case is of low intensity, the pattern of relative frequencies and intensities is remarkably close.

(13) Koelle, U. *J. Organomet. Chem.* **1978**, *155*, 53.

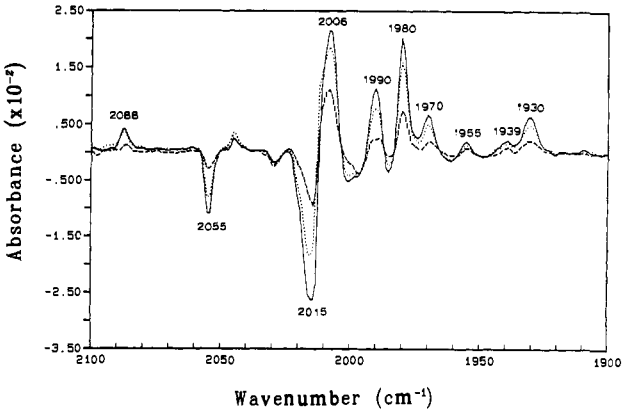

Figure 2. Difference IR spectra of the same sample in the same experiment as in Figure 1 (with the spectrum taken at 30 min after the flashes as the reference). They show the differences between the spectra obtained at 80 (---), 140 (···), and 180 min (—) after the flashes and the spectrum at 30 min, respectively. Not included in this figure is the band at 1760 cm^{-1}, which shows a gradual decline in intensity along with other peaks, such as those at 2055 and 2016 cm^{-1}.

We propose that the transient bands are due to a solvent-coordinated species, $Mn_2(CO)_9(S)$ (S = solvent), formed as an alternative to the semibridged species when a solvent molecule is in an optimal position with respect to the vacant site on Mn in the thermally equilibrated CO-loss product. It is well-known that hydrocarbon solvent molecules can bind to 16-electron metal centers, e.g., in $Cr(CO)_5$.[14] The fact that the semibridging form of $Mn_2(CO)_9$* is the prevalent form in fluid hydrocarbon solution indicates that it is more stable than a solvent-coordinated species.[6a,15] At 90 K, however, if the solvent-coordinated species were kinetically favored, it would be expected to persist for some time before displacement by a CO from the adjacent metal to form the semibridged species.

Another group of peaks, observed immediately after the photolysis, grows slowly, accompanied by the continuous decline of the solvent-coordinated species (Figure 1) as well as the semibridged intermediate. Figure 2 shows the decay of the semibridged species and the concurrent formation of the new absorption bands. The apparent conversion is accelerated when the sample is warmed slowly to around 120 K. Eventually $Mn_2(CO)_9$* completely disappears, as indicated by disappearance of the peak at 1760 cm^{-1}, leaving only the product with absorbances at 2088, 2006, 1990, 1980, 1970, 1955, 1939, and 1930 cm^{-1}.

To avoid the complexity of secondary photolysis arising from multiple flashes, a freshly prepared solution sample with identical composition was photolyzed with only a single flash at 143 K. At this temperature, the 3-methylpentane medium is still quasi-glassy, and diffusional processes are limited, except for small solutes such as CO. The difference spectra reveal principally the same absorption bands with similar intensities. Very few changes are observed over a period of 30 min. The absence of absorbance at 1760 cm^{-1} indicates completion of $Mn_2(CO)_9$* conversion in less than 1 or 2 min at 143 K. In the experiments at both 90 and 143 K, reactions associated with the $Mn(CO)_5$ radicals are not expected and apparently not observed. In a frozen matrix, characteristic of the 90 K experiments, the radicals produced via metal–metal bond homolysis normally recombine quickly in the solvent cage. Even at 143 K, escape of $Mn(CO)_5$ radicals from the cage appears to be very limited; there is little or no evidence of products that might form from diffusively separated radicals, e.g., $Mn_2(CO)_8[P(n\text{-}Bu)_3]_2$.

When the irradiated samples were warmed to room temperature, the IR spectra showed absorbance bands at 2090, 2008, 1990,

(14) (a) Perutz, R. N.; Turner, J. J. *J. Am. Chem. Soc.* **1975**, *97*, 4791. (b) Lee, M.; Harris, C. B. *J. Am. Chem. Soc.* **1989**, *111*, 8963. (c) Simon, J. D.; Xie, X. *J. Phys. Chem.* **1986**, *90*, 6751; **1987**, *91*, 5538; **1989**, *93*, 291. (d) Zhang, S.; Dobson, G. R.; Zang, V.; Bajaj, H. C.; van Eldik, R. *Inorg. Chem.* **1990**, *29*, 3477.

(15) Zhang, J. Z.; Harris, C. B. *J. Chem. Phys.* **1991**, *95*, 4024.

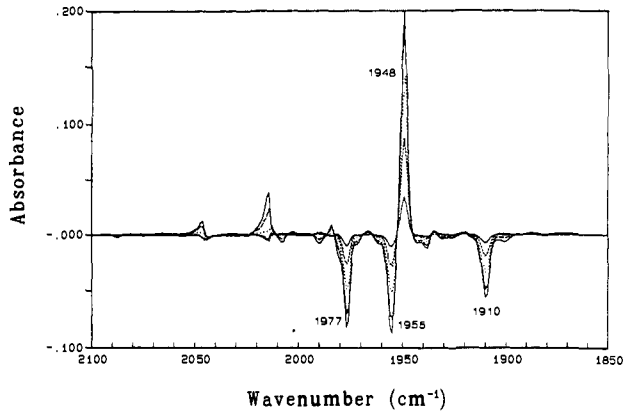

Figure 3. Difference spectra of a mixed solution of 3-methylpentane and hexane (2:1 by volume) containing 4.9×10^{-4} M $Mn_2(CO)_{10}$ and 4.2×10^{-3} M $P(n\text{-}Bu)_3$ after photolysis at 213 K with liquid nitrogen as the coolant. They show the differences between the spectra acquired at 3, 6, 12, 20, and 30 min (in upward order for the upper half or downward for the lower half) and the reference spectrum, obtained at 1 min after the photolysis.

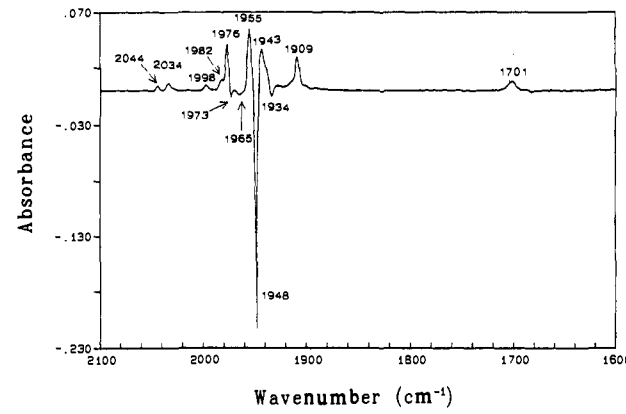

Figure 4. IR difference spectrum of a 3-methylpentane solution of 7.1×10^{-4} M $Mn_2(CO)_8[P(n\text{-}Bu)_3]_2$ subjected to a single flash while maintained at 173 K. The absorbance difference is between the spectra taken 1 min after photolysis and the one taken before the flash.

1970, 1941, and 1933 cm^{-1}. A few changes are obvious: the 1980-cm^{-1} band disappears, the 1990-cm^{-1} band becomes much stronger, and the 1933-cm^{-1} band increases moderately, while others, such as those at 2088, 2008, 1972, 1955, and 1941 cm^{-1}, show weaker intensities and small position shifts. A new solution sample was flashed once at 243 K, and the IR spectra were recorded subsequently at regular intervals. Except for the peak at 1949 cm^{-1}, assigned to the disubstituted compound, $Mn_2(CO)_8[P(n\text{-}Bu)_3]_2$, other bands are in the same positions as at lower temperature and they show similar changes as described above.

By comparison with the IR spectra of other monosubstituted compounds, such as *e*-$Mn_2(CO)_9py$ and *a*-$Mn_2(CO)_9PPh_3$ (Table I),[13] it is reasonable to conclude that the species formed at lower temperature giving rise to the absorbance band at 1980 cm^{-1} is the equatorial isomer, *e*-$Mn_2(CO)_9P(n\text{-}Bu)_3$. This species remains unchanged until the temperature is raised to about 240 K, at which temperature it undergoes isomerization to convert to the thermodynamically more favorable axially-substituted isomer, *a*-$Mn_2(CO)_9P(n\text{-}Bu)_3$, in approximately 1 h.

A set of new absorbance bands was discovered using a similar solution sample photolyzed at 213 K. The difference spectrum for the sample immediately after the flash reveals bands at 1977, 1955, and 1910 cm^{-1} in addition to the bands already known for *e*-$Mn_2(CO)_9P(n\text{-}Bu)_3$ and *a,a*-$Mn_2(CO)_8[P(n\text{-}Bu)_3]_2$.[16] Given the high rate constants for radical recombination at room temperature, it is to be expected that at 213 K the radicals will have recombined before the first IR measurement is taken following flash irradiation. Thus, the three new bands are characteristic of the products of radical recombination, rather than of the radicals themselves. The intensities of the three bands gradually decrease, concurrent with growth of the band at 1948 cm^{-1}, assigned to *a,a*-$Mn_2(CO)_8[P(n\text{-}Bu)_3]_2$ (Figure 3). These observations point to a new intermediate that undergoes reaction to yield *a,a*-$Mn_2(CO)_8[P(n\text{-}Bu)_3]_2$ as the sole product. The pattern of IR frequencies and relative intensities of the new intermediate is closely analogous to that of diequatorially-substituted compounds, e.g., *e,e*-$Mn_2(CO)_8(PMe_3)_2$ (see Table I for more detailed listing).[17] Thus, the new species is assigned as *e,e*-$Mn_2(CO)_8[P(n\text{-}Bu)_3]_2$, formed via recombination of $Mn(CO)_4P(n\text{-}Bu)_3$ radicals.

Similar experiments were conducted with $P(i\text{-}Bu)_3$ as the substituting ligand. The *e*-$Mn_2(CO)_9P(i\text{-}Bu)_3$ intermediate, which has IR absorption frequencies nearly identical to those for the $P(n\text{-}Bu)_3$ analogue, is the kinetic product. It undergoes further isomerization to the axially-substituted compound. Because $P(i\text{-}Bu)_3$ is bulkier than $P(n\text{-}Bu)_3$, significant differences are seen in the two systems. There is far less disubstituted product in the $P(i\text{-}Bu)_3$ case. The disubstituted compound exists in comparable amounts with the monosubstituted only when the photolysis is conducted at a temperature around or higher than 273 K, presumably because phosphine substitution of the radicals is comparatively slower in relationship to recombination of $Mn(CO)_5$ radicals. In addition, the temperature at which the isomerizations occur is generally higher than when $P(n\text{-}Bu)_3$ is used. Possible reactions for a solution of $Mn_2(CO)_{10}$ and substituting ligand L following photolysis are shown in Scheme I.

Scheme I

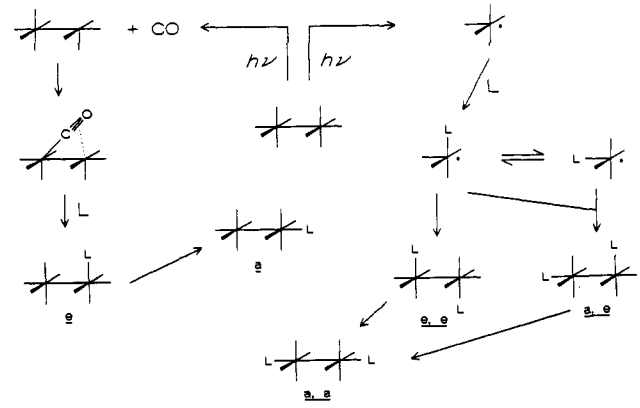

Low-Temperature Flash Photolyses of $Mn_2(CO)_8L_2$ Solutions. 3-Methylpentane solutions of $Mn_2(CO)_8[P(n\text{-}Bu)_3]_2$ were flash-irradiated under conditions similar to those described above, with IR spectral detection to monitor the dynamic processes following photolysis. Difference spectra were obtained following a single flash while the sample was maintained at 173 K. Among the new absorbance peaks resulting from photolysis, most notable is the absorption at 1701 cm^{-1}, associated with the semibridging CO ligand and thus characteristic of the CO-loss product, $Mn_2(CO)_7[P(n\text{-}Bu)_3]_2$*, and the absorptions at 1976, 1955, and 1909 cm^{-1}, assigned on the basis of experiments described above to the diequatorially-substituted isomer, *e,e*-$Mn_2(CO)_8[P(n\text{-}Bu)_3]_2$ (Figure 4). The 1701-cm^{-1} band intensity decreases over a period of about 1 h, while the temperature is maintained at 173 K. At the same time, two weaker absorptions at 1715 and 1687 cm^{-1} appear, indicating a conversion of the semibridged species formed at the flash to new intermediates also containing semibridging CO ligands.

Through observation of the photolysis of solutions containing $Mn_2(CO)_{10}$ and $P(n\text{-}Bu)_3$ (vide supra), it appears that conversion of *e,e*-$Mn_2(CO)_8[P(n\text{-}Bu)_3]_2$ to the a,a-isomer proceeds at around 210 K. It is therefore reasonable to assume that the changes occurring in other absorption bands at 173 K, accompanying the decline in absorbance at 1701 cm^{-1}, are associated entirely with the reaction involving the semibridged intermediate, Mn_2-

(16) Lewis, J.; Manning, A. R.; Miller, J. R. *J. Chem. Soc. A* **1966**, 845.
(17) Reimann, R. H.; Singleton, E. *J. Chem. Soc., Dalton Trans.* **1976**, 2109.

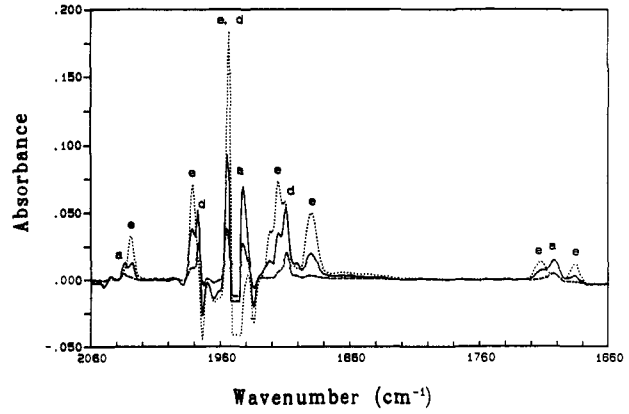

Figure 5. Differences between the IR spectra obtained after and before photolysis of $Mn_2(CO)_8[P(n\text{-}Bu)_3]_2$ in 3-methylpentane solution maintained at 173 K. They were obtained after a single flash (---), after 10 flashes (—) and after 30 flashes (···), respectively. The peaks marked with a, e, and d are assigned to $a,a\text{-}Mn_2(CO)_7[P(n\text{-}Bu)_3]_2$*, $a,e\text{-}Mn_2(CO)_7[P(n\text{-}Bu)_3]_2$*, and $e,e\text{-}Mn_2(CO)_8[P(n\text{-}Bu)_3]_2$, respectively.

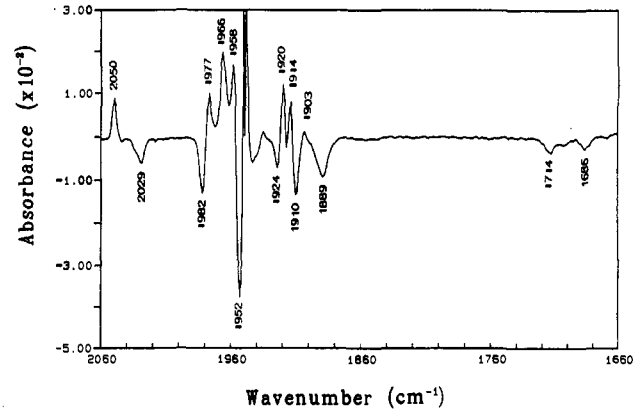

Figure 6. Difference spectrum of a 7.1×10^{-4} M $Mn_2(CO)_8[P(n\text{-}Bu)_3]_2$ solution in 3-methylpentane subjected to a single flash while maintained at 213 K with dry ice/acetone as refrigerant. The IR absorbance difference is between the spectra taken at 5 min and 1 min after photolysis.

$(CO)_7[P(n\text{-}Bu)_3]_2$*. On the basis of the difference spectra, it can be concluded that the initial semibridged species $Mn_2(CO)_7[P(n\text{-}Bu)_3]_2$* has absorption peaks at 2035, 1976, 1944, 1902, and 1701 cm^{-1}. The newly-formed species are characterized by bands at 2029, 1981, 1952, 1915, 1889, 1715, and 1687 cm^{-1}. These assignments leave uncertain the origins of two peaks at 2044 and 1998 cm^{-1} in Figure 4; they are not associated with any of the intermediates mentioned.

Apparently the kinetic product of CO loss undergoes a facile subsequent isomerization to yield two distinct successor products which retain the semibridge. The first kinetic product formed on photolysis is likely to have a structure with the substituent ligands in axial positions, as is characteristic of the starting material. In the isomerized species, at least one phosphine ligand is likely to occupy an equatorial position, either cis or trans with respect to the semibridging bond. As a means of further characterizing these isomers, a 3-methylpentane solution of $a,a\text{-}Mn_2(CO)_8[P(n\text{-}Bu)_3]_2$ at 173 K was subjected to a single flash. As expected, IR bands due to the kinetic product of CO loss, as well as those due to $e,e\text{-}Mn_2(CO)_8[P(n\text{-}Bu)_3]_2$, were observed. This solution was then subjected to multiple-flash irradiations. Shown in Figure 5 are the representative spectra taken during such a process. Initially, along with consumption of the starting material as the result of photolysis, indicated by the decaying peak at 1948 cm^{-1}, the band at 1701 cm^{-1} grows, accompanied by the bands at 1715 and 1687 cm^{-1}, as well as the bands for $e,e\text{-}Mn_2(CO)_8[P(n\text{-}Bu)_3]_2$. With more flashes the 1948-cm^{-1} band continues to decay; the 1701-cm^{-1} band completely disappears, while the 1715- and 1687-cm^{-1} bands increase. Judging from the intensity change of the 1909-cm^{-1} peak, which is less overlapped than other absorptions, the amount of $e,e\text{-}Mn_2(CO)_8[P(n\text{-}Bu)_3]_2$ decreases, instead of growing as expected. Our interpretation of these results is that the kinetic CO-loss product undergoes isomerization to the two successor semibridging forms, while $e,e\text{-}Mn_2(CO)_8[P(n\text{-}Bu)_3]_2$ undergoes CO loss under photolysis to yield one or the other of the same two isomers. Isomerization among the semibridging intermediates apparently occurs much faster than previously observed under thermal conditions.

We do not have sufficient information to fully elucidate the geometries of the isomers; however, a plausible scheme is shown as Scheme II. For convenience in the following discussion, the two semibridging isomers giving rise to the bands at 1715 and 1686 cm^{-1} are referred to collectively as $a,e\text{-}Mn_2(CO)_7[P(n\text{-}Bu)_3]_2$*. Isomerization of a CO-loss product has been studied before, with $Re_2(CO)_{10}$ subjected to 313-nm photolysis in low-temperature matrices.[1d] It was found that $e\text{-}Re_2(CO)_9(Ar)$, initially generated via photolysis in the Ar matrix, isomerizes to the a-isomer under 546-nm irradiation.

A single-flash photolysis of $a,a\text{-}Mn_2(CO)_8[P(n\text{-}Bu)_3]_2$ was carried out at a higher temperature, 213 K. In contrast to the observation made at lower temperature, $a,e\text{-}Mn_2(CO)_7[P(n\text{-}Bu)_3]_2$*, with the characteristic semibridging CO absorption peaks at 1714 and 1686 cm^{-1}, is the dominant CO-loss product in solution immediately after photolysis; on the other hand, only a small amount of $e,e\text{-}Mn_2(CO)_7[P(n\text{-}Bu)_3]_2$* exists. It quickly disappears, as determined from the decline in peak intensity at 1701 cm^{-1}. The decay of the a,e-semibridged intermediates takes about 10 min. At this temperature, the $e,e\text{-}Mn_2(CO)_8[P(n\text{-}Bu)_3]_2$ formed following the flash has largely converted to the stable diaxial isomer. Accompanying the decay of $a,e\text{-}Mn_2(CO)_7[P(n\text{-}Bu)_3]_2$* are increases in absorbances at 2050, 1977, 1966, 1958, 1920, 1914, and 1903 cm^{-1} (Figure 6), already present in the solution when the initial measurement is taken. It is evident that $a,e\text{-}Mn_2(CO)_7[P(n\text{-}Bu)_3]_2$* is responsible for product peaks other than those assignable to $a,a\text{-}Mn_2(CO)_8[P(n\text{-}Bu)_3]_2$, because $e,e\text{-}Mn_2(CO)_8[P(n\text{-}Bu)_3]_2$ converts solely to the a,a-isomer, as demonstrated before. (In this difference IR spectrum, two peaks at 1924 and 1910 cm^{-1} appear, instead of a single peak at the position of the 1915-cm^{-1} band for $a,e\text{-}Mn_2(CO)_7[P(n\text{-}Bu)_3]_2$*. The apparent peak splitting results from overlap with the growing CO-recombination product peaks at 1920 and 1914 cm^{-1}.)

Scheme II

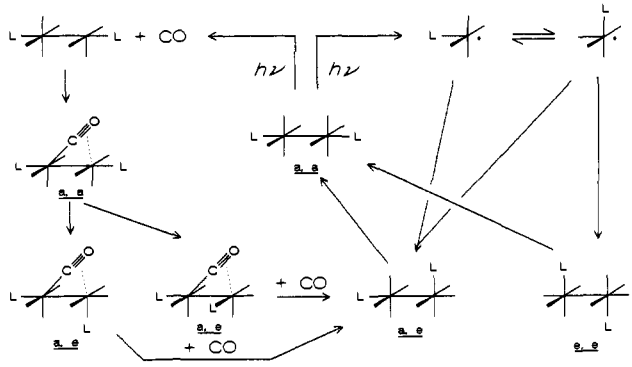

To study the behavior of the new species more clearly, IR spectra were obtained in a similar manner at 243 K with a freshly prepared solution sample. At this temperature, isomerizations of both $e,e\text{-}Mn_2(CO)_8[P(n\text{-}Bu)_3]_2$ and $a,a\text{-}Mn_2(CO)_7[P(n\text{-}Bu)_3]_2$*, yielding $a,a\text{-}Mn_2(CO)_8[P(n\text{-}Bu)_3]_2$ and $a,e\text{-}Mn_2(CO)_7[P(n\text{-}Bu)_3]_2$*, respectively, are expected to be complete in less than a few minutes. Thus, the only feasible source of the absorption bands seen at 2050, 1977, 1966, 1957, 1920, 1914, 1904, and 1891 cm^{-1} is a product of the reaction of CO with $a,e\text{-}Mn_2(CO)_7[P(n\text{-}Bu)_3]_2$*. This product gradually converts to the starting material $a,a\text{-}Mn_2(CO)_8[P(n\text{-}Bu)_3]_2$ over 40 min at 243 K. The absence of bands ascribable to semibridging CO, and the fact that the intermediate converts to the starting material, leads to the assignment of $a,e\text{-}Mn_2(CO)_8[P(n\text{-}Bu)_3]_2$ for the new intermediate. It is presumed to form via reaction of $a,e\text{-}Mn_2(CO)_7[P(n\text{-}Bu)_3]_2$*

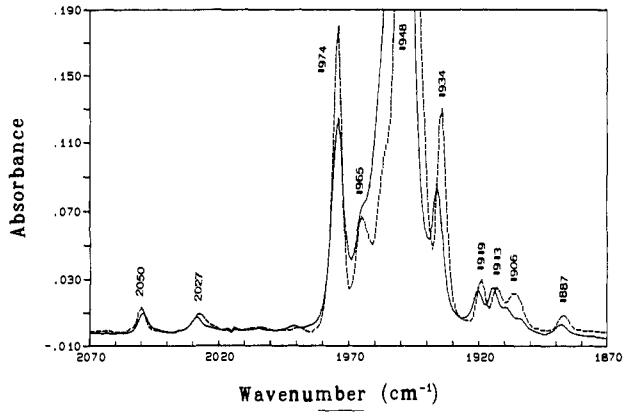

Figure 7. IR spectra of a 7.1×10^{-4} M $Mn_2(CO)_8[P(n\text{-}Bu)_3]_2$ solution in 3-methylpentane, at room temperature (—) and 173 K (---).

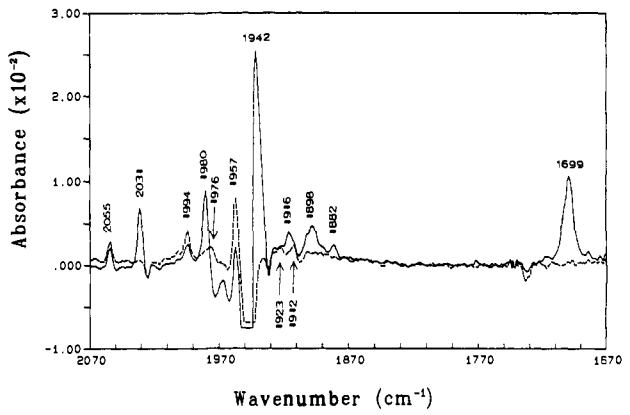

Figure 8. Difference spectra of $Mn_2(CO)_8[PCy_3]_2$ in 3-methylpentane solution after a single-flash photolysis at room temperature. The spectrum of the solution before photolysis serves as reference. The spectra were obtained at 0.5 (—) and 6 (---) min, respectively, after photolysis.

with CO. The a,e-type isomers are known in the Re analogues, e.g., $Re_2(CO)_8L_2$ (L = $P(n\text{-}Bu)_3$ and PPh_3) (Table I).[3f] The IR band patterns of a,e-isomers are similar for manganese and rhenium carbonyls.

It is noteworthy that, in the room-temperature IR solution spectrum of $Mn_2(CO)_8[P(n\text{-}Bu)_3]_2$, in addition to the major bands at 1974, 1950, and 1936 cm^{-1}, assigned to $a,a\text{-}Mn_2(CO)_8[P(n\text{-}Bu)_3]_2$, much weaker peaks are found at 2045, 2027, 1921, 1913, 1906, and 1887 cm^{-1} (Figure 7). The intensities are only about 1% of the 1950-cm^{-1} band intensity. (In the same solution at 173 K, an additional absorption at 1965 cm^{-1} is clearly visible. At the lower temperature, the bands are narrower and thus more clearly discernable.) The match of these bands to those assigned to the putative $a,e\text{-}Mn_2(CO)_8[P(n\text{-}Bu)_3]_2$ suggests that there is a thermal equilibrium between the a,a- and a,e-isomers, with the less stable a,e-form present to the extent of about 1%. Given that $Mn_2(CO)_8[PMe_3]_2$ exists in solution predominantly in the e,e-form, it is quite reasonable that the energy difference between the a,a- and a,e-isomeric forms of $Mn_2(CO)_8[P(n\text{-}Bu)_3]_2$ should be fairly small. It was proposed in earlier work that certain of the weak bands which we ascribe to the a,e-isomer are due to ^{13}CO-substituted $a,a\text{-}Mn_2(CO)_8[P(n\text{-}Bu)_3]_2$.[16] Those assignments may indeed be correct; however, the peaks at 1914 and 1919 cm^{-1} in the spectra of $Mn_2(CO)_8[P(n\text{-}Bu)_3]_2$ could not be so assigned. These bands disappear in concert with the others we ascribe to the a,e-isomer. Thus, the ^{13}CO bands and certain bands due to the a,e-isomer probably coincide.

Flash photolyses of 3-methylpentane solutions of $Mn_2(CO)_8(PCy_3)_2$ at 213 K yield difference IR spectra which exhibit no evidence of the e,e-isomeric form. Instead, they reveal a band at 1699 cm^{-1} for the semibridging CO ligand in $Mn_2(CO)_7(PCy_3)_2$*, characteristic of CO loss, and other terminal CO bands at higher frequencies. Very little change with time is observed in the spectra at 213 K. In fact, the CO-loss product persists for a few minutes at room temperature, an indication of dramatically slower recombination with CO than for smaller phosphines. On the basis of data acquired at 300 K, the absorption frequencies for the semibridged $Mn_2(CO)_7(PCy_3)_2$* are 2031, 1980, 1942, 1916, 1898, 1882, and 1699 cm^{-1}. The bands decay in a few minutes following photolysis; recombination with CO leads to the starting material, as evidenced by the growth in absorbance at 1947 cm^{-1}. Additional absorption bands are observed at 2055, 1994, 1976, 1957, 1923, and 1912 cm^{-1} at the beginning of the data acquisition process. Their intensities are smaller than those of the semibridging intermediate. A few of them are overlapped by the semibridging intermediate, and their identification is only possible after its decay (Figure 8). Except for the band at 1994 cm^{-1}, discussed in the next paragraph, these are likely due to a species formed independently of the CO-loss product. Their intensities change little over 1 h or longer. On the basis of the IR band pattern, they could be due to the a,e-isomer, which might be formed via recombination of $Mn(CO)_4PCy_3$ radicals. An additional feature associated with $Mn_2(CO)_8(PCy_3)_2$ photolysis is that the 1699-cm^{-1} band of the initally-formed semibridge form shows no conversion to other peaks, such as those at 1717 and 1686 cm^{-1} in the case of $Mn_2(CO)_8[P(n\text{-}Bu)_3]_2$. A similar experiment was conducted at 273 K, also with the appearance of the semibridging CO peak at 1699 cm^{-1} as the result of photolysis. This band shows similar behavior: only an intensity decrease without conversion to other bands attributable to different semibridged intermediates. The fact that PCy_3 is a much bulkier ligand than $P(n\text{-}Bu)_3$ suggests that configurations with a ligand at any position other than axial are thermodynamically unfavorable.

The intensity of the 1994-cm^{-1} band, present immediately after the photolysis, shows a very slow increase over time. The process lasts for a few days, accompanied by increases in other absorbances and by a loss of starting material. The slow conversion results in complete depletion of the starting material within a few days. The resulting solution shows IR bands at 2089, 2026, 2015, 2002, 1994, 1973, 1957, 1942, 1929, 1921, and 1911 cm^{-1}. The major component is the monosubstituted compound, $a\text{-}Mn_2(CO)_9(PCy_3)$. Since the same reaction does not occur under the same conditions for a solution that has not been subjected to flash photolysis, it is reasonable to assume that the reaction involves replacement of a PCy_3 in the starting material by free CO released upon decomposition caused by the flash.

A 3-methylpentane solution of $Mn_2(CO)_8(PCy_3)_2$ in a laser photolysis cell was degassed and brought up 1 atm of CO as cover gas. The solution was kept in the dark except for momentary exposure to the room light when UV–visible spectra were taken. The solution absorbance peak shifted to shorter wavelength in 1 day and then remained unchanged. The difference spectra show that the decaying peaks are at 456 and 388 nm. The IR spectrum further reveals peaks at 2089, 2025, 2002, 1994, 1973, 1957, 1943, 1929, 1922, and 1908 cm^{-1}. The spectrum is nearly identical with the spectra obtained with the sample subjected to flash lamp irradiation, except for the absence of the 2015-cm^{-1} absorption band. Those facts suggest that a slow thermal reaction occurs between $Mn_2(CO)_8(PCy_3)_2$ and free CO ligand and that the product is the monosubstituted species. The reaction is probably CO-concentration-dependent; under 1 atm of CO it is virtually complete within 1 day, while, in the flash-photolyzed solution, in which the free CO concentration is much smaller, the reaction occurs over a few days.

$Mn_2(CO)_8[P(i\text{-}Pr)_3]_2$ shows similar behavior under photolysis. At room temperature a single-flash irradiation of a 3-methylpentane solution of $Mn_2(CO)_8[P(i\text{-}Pr)_3]_2$ leads to formation of the semibridged species $a,a\text{-}Mn_2(CO)_7[P(i\text{-}Pr)_3]_2$*, which recombines with CO in a few minutes to regenerate the starting compound, as evidenced by the loss in intensity of the band at 1701 cm^{-1}. Bands at 2033, 1980, 1945, and 1902 cm^{-1} are also assignable to this intermediate, as they disappear concurrently with the band at 1701 cm^{-1}. A few fands are not yet accounted for: 2057, 1996, 1978, 1959, and 1930 cm^{-1}, which are also present in the case of $Mn_2(CO)_8(PCy_3)_2$. Among them the 2057-, 1978-,

and 1959-cm^{-1} bands are possibly due to the a,e-isomer, formed via a radical process. Others, notably the 1995-cm^{-1} band, which slowly increases over a long period of time, are ascribable to the monosubstituted compound.

The most stable isomeric form for $Mn_2(CO)_8(PMe_3)_2$ is the e,e-isomer. Upon flash photolysis of $Mn_2(CO)_8(PMe_3)_2$ at 173 K, the majority of new bands seen are those due to the CO-loss product $Mn_2(CO)_7(PMe_3)_2$*. From the difference spectra, monitoring concurrent decreases in absorption bands, its absorption frequencies can be assigned as 2031, 1986, 1955, 1929, 1887, and 1717 cm^{-1}. A very weak absorption at 1692 cm^{-1} may also be assignable to this species. The observed frequency (or frequencies) for the semibridge species suggests one or possibly two "equatorial" locations for PMe_3 in the semibridged form. The peak position here provides support for the structures assigned to the more stable isomeric forms of $Mn_2(CO)_7[P(n\text{-}Bu)_3]_2$*.

The product formed as the result of the disappearance of the semibridged compound exhibits IR bands at 2053, 2007, 1961, 1942, 1917, 1905, and 1863 cm^{-1}, consistent with initial formation of the a,e-isomer as a dominant product. Some of the peaks are broad, specially the bands at 1905 and 1863 cm^{-1}. When the solution is warmed to room temperature, the IR spectrum is virtually the same as that obtained before photolysis, indicating conversion of the a,e-isomer to the e,e-isomeric starting material.

UV–Visible Spectra of Intermediates. The transient spectra of active intermediates are obtained via laser pulse photolysis coupled with a fast-response diode array UV–visible detection. The two primary photoproducts of photolysis of $Mn_2(CO)_{10}$, the semibridged $Mn_2(CO)_9$* and the radical $Mn(CO)_5$·, were determined in this way to absorb in the vicinity of 500 and 800 nm, respectively.[18] Our data are in agreement with earlier findings. The absorbance maxima for the analogous photoproducts formed from the disubstituted compounds are found in these regions as well by applying pulsed laser flash spectroscopy; for example, $Mn_2(CO)_7[P(n\text{-}Bu)_3]_2$* absorbs at about 530 nm. In addition, *a,e*-$Mn_2(CO)_8[P(n\text{-}Bu)_3]_2$ absorbs at 420 nm, and the e,e-isomer at 470 nm. The band corresponding to the a,e-isomer was first reported by Kobayashi and co-workers. In addition they noted a transient species with an absorption maximum at 470 nm; however, they were not able to assign it to the e,e-isomeric form.[19]

To obtain the UV–visible spectra for the intermediates, the low-temperature IR cell assembly was used as if it were a UV–visible cell. After photolysis, the cell assembly is quickly transferred to a UV–visible spectrometer, and spectra are recorded. The IR spectra are obtained as well, so that the species formed in the photolyses can be identified unambiguously. Since the temperature can be controlled at various levels, the UV–visible spectra of certain intermediates, and their transformations, can be elucidated as in the IR study.

A solution containing 5.0×10^{-4} M $Mn_2(CO)_{10}$ and 3.3×10^{-2} M $P(i\text{-}Bu)_3$ was photolyzed with a single flash with the temperature maintained at 213 K. The solution was further warmed to room temperature about 40 min later and then cooled to 213 K again. The IR and UV–visible spectra were acquired during this process. The difference IR spectrum after photolysis at 213 K shows predominant formation of *e*-$Mn_2(CO)_9P(i\text{-}Bu)_3$. Its transformation to the axial isomer occurs slowly at 213 K; the process is completed upon warming to room temperature, at which point a small amount of diaxially-substituted compound is present, in addition to the much larger amount of *a*-$Mn_2(CO)_9P(i\text{-}Bu)_3$. The solution is subsequently cooled to 213 K merely to take advantage of a constant background for both IR and UV–visible spectral measurements.

Figure 9 shows UV–visible absorbance spectra of such a sample after photolysis. Respectively, they correspond to *e*- and *a*-$Mn_2(CO)_9P(i\text{-}Bu)_3$. The band at around 420 nm declines slowly and shifts to slightly shorter wavelength when the isomerization

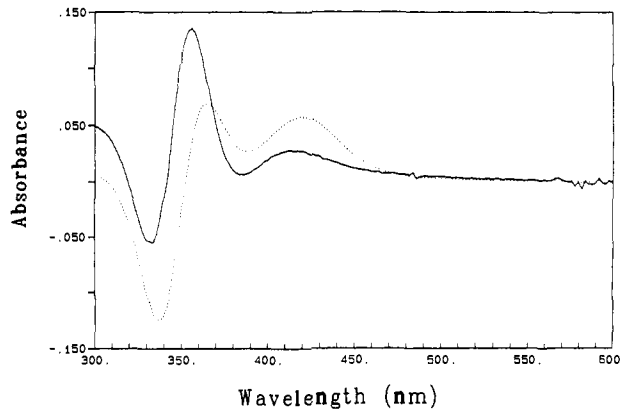

Figure 9. Difference UV–visible spectra of a 3-methylpentane solution containing 5.4×10^{-4} M $Mn_2(CO)_{10}$ and 3.3×10^{-2} M $P(i\text{-}Bu)_3$ after photolysis with a single flash at 213 K with the spectrum before the flash as the reference. One spectrum (···) was obtained at 213 K shortly after the photolysis; the other (—) was taken after the temperature of the photolyzed solution was first raised to room temperature and then cooled back to 213 K.

is complete. Therefore the absorbance peaks for *e*- and *a*-$Mn_2(CO)_9P(i\text{-}Bu)_3$ in the 400-nm region are at 420 and 414 nm, respectively.

The $P(n\text{-}Bu)_3$-substituted intermediate spectra were obtained in a similar way. Special efforts were made to control temperature, as both *e*-$Mn_2(CO)_9P(n\text{-}Bu)_3$ and *e,e*-$Mn_2(CO)_8[P(n\text{-}Bu)_3]_2$ normally form in comparable amounts. Typically, a solution containing 5.0×10^{-4} M $Mn_2(CO)_{10}$ and 1.7×10^{-2} M $P(n\text{-}Bu)_3$ is flashed once at 203 K. The IR spectrum shows that the diequatorially-substituted intermediate quickly converts to the diaxial isomer, while the monosubstituted equatorial compound is fairly stable at that temperature. In this case, then, the UV–visible difference spectrum is attributable mainly to *e*-$Mn_2(CO)_9P(n\text{-}Bu)_3$. The absorbance maximum occurs at about 420 nm; a value nearly identical to that seen for the $P(i\text{-}Bu)_3$ analogue. When a solution of the same initial composition is photolyzed at 193 K, both equatorially-substituted compounds, *e*-$Mn_2(CO)_9P(n\text{-}Bu)_3$ and *e,e*-$Mn(CO)_8[P(n\text{-}Bu)_3]_2$, are generated and sufficiently long-lived for spectroscopic measurement. A peak at 440 nm is revealed after the photolysis. As the position for the monosubstituted species has been determined, the 440-nm absorbance is assigned to *e,e*-$Mn_2(CO)_8[P(n\text{-}Bu)_3]_2$.

Room-Temperature Flash Photolysis. Having reliable values for absorbance maxima associated with the various intermediates, it is feasible to measure their transient behaviors. Pulsed laser or Xenon lamp flash photolysis at room temperature, with UV–visible detection, provides a means of observing transients identified with the various species formed initially or secondarily following flash photolysis.

The kinetics of *e*-$Mn_2(CO)_9P(n\text{-}Bu)_3$ isomerization were studied by monitoring the transient decay feature at 420 nm in hexane solutions containing $Mn_2(CO)_{10}$ and excess ligand, subjected to 308-nm laser pulse photolyses, as shown in Figure 10. The graph of ln *A* vs time shown in the inset is linear, demonstrating that the decay is first order. Because the intermediate is the initial product of reaction between the added ligand and semibridged species, its concentration cannot readily be accurately determined. However, an estimate of relative initial concentrations can be made on the basis of the total absorbance change in the isomerization process. The observed rate constants show no evidence of a dependence on concentration of either *e*-$Mn_2(CO)_9P(n\text{-}Bu)_3$ or the ligand. An average rate constant of 12.5 s^{-1} is found for the *e*-$Mn_2(CO)_9P(n\text{-}Bu)_3 \rightarrow$ *a*-$Mn_2(CO)_9P(n\text{-}Bu)_3$ process at 24 °C.

Just as *e,e*-$Mn_2(CO)_8[P(n\text{-}Bu)_3]_2$ can be produced by photolyzing either solutions of *a,a*-$Mn_2(CO)_8[P(n\text{-}Bu)_3]_2$ or mixtures of $Mn_2(CO)_{10}$ and $P(n\text{-}Bu)_3$, its isomerization can be studied by following the decay in absorbance at 460–470 nm in either kind of solution after flash photolysis. An observed first-order rate constant of 1.54×10^3 s^{-1} for decay of the transient at 470 nm

(18) Rothberg, L. J.; Cooper, N. J.; Peters, K. S.; Vaida, V. *J. Am. Chem. Soc.* **1982**, *104*, 3536.
(19) Yasufuku, K.; Hiraga, N.; Ichimura, K.; Kobayashi, T. *Coord. Chem. Rev.* **1990**, *97*, 167.

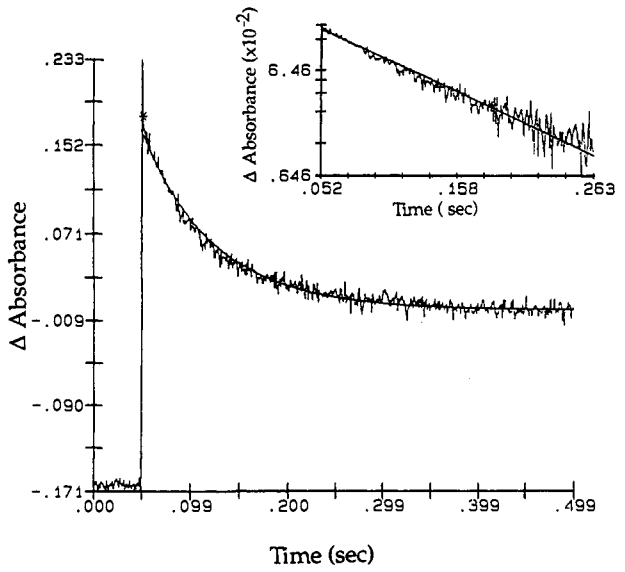

Figure 10. Transient absorbance decay (average of 10) at 420 nm of a hexane solution containing 4.9×10^{-4} M $Mn_2(CO)_{10}$ and 9.79×10^{-2} M P(*n*-Bu)$_3$ after single-laser-pulse excitations at 308 nm. The insertion shows the plot of ln (Abs) vs time.

was determined with a hexane solution containing 4.9×10^{-4} M $Mn_2(CO)_{10}$ and 9.79×10^{-2} M P(*n*-Bu)$_3$ after laser pulse excitation at 308 nm. However, in the shorter time interval preceding the decay, we observed a faster process leading to an increase in absorbance at 470 nm. The faster step is attributed to coupling of the basally-substituted $Mn(CO)_4P(n\text{-}Bu_3)$ radicals, formed by facile ligand substitution of the primary metal–metal bond homolysis product, the $Mn(CO)_5$ radical.

Photolyses of $Mn_2(CO)_8[P(n\text{-}Bu)_3]_2$ solutions were conducted using a conventional xenon flash lamp apparatus. As with the laser flash experiment, the absorbance in the 460–470-nm region exhibits an initial increase and then a decay, corresponding respectively to the formation and subsequent isomerization of *e,e*-$Mn_2(CO)_8[P(n\text{-}Bu)_3]_2$. However, in the xenon flash experiments, the absorbance increase is masked in part by the trailing edge of the flash pulse. Furthermore, the longer time behavior of the transient indicates an additional, much slower step that gives rise to a comparatively small absorbance decrease. This slow process is due to CO recombination with the semibridged species; there is a small absorbance at 470 nm from the band which has its maximum at 530 nm. This slow process does not present difficulty in the measurement of the much faster isomerization step.

The observed first-order rate constants obtained for the isomerization process are listed in Table II for several initial concentrations of $Mn_2(CO)_8[P(n\text{-}Bu)_3]_2$ and $Mn_2(CO)_8[P(i\text{-}Bu)_3]_2$. The apparent first-order rate constant increases with increasing concentration of the dimer and then appears to level off, at least in the case of P(*n*-Bu)$_3$, for which the data are more extensive. The origin of this effect is the partial overlap in the time domain with recombination of the $Mn(CO)_4L$ radicals, giving rise to *e,e*-$Mn(CO)_8L_2$, with subsequent isomerization to *a,a*-$Mn_2(CO)_8L_2$. Because the radical recombination reaction is second order, it decays more gradually than the first-order process, and its half-life is concentration-dependent. The result is that, for the most dilute solutions, relatively more radical recombination is occurring during the early stages of the e,e → a,a isomerization. The product of the radical recombination is *e,e*-$Mn_2(CO)_8L_2$. Thus, the reaction system is as follows:

$$2Mn(CO)_4L \rightarrow e,e\text{-}Mn_2(CO)_8L_2 \quad (1)$$

$$e,e\text{-}Mn_2(CO)_8L_2 \rightarrow a,a\text{-}Mn_2(CO)_8L_2 \quad (2)$$

Numerical simulation of the system shows the effect observed: an apparently lower first-order rate constant at lower initial concentrations of the dimer, converging to a constant value as the dimer concentration increases.[20]

Table II. Observed Rate Constants for the e,e to a,a Isomerization in Hexane Solutions of $Mn_2(CO)_8L_2$ under Ar Atmosphere

k_{obsd} (s^{-1})	$[Mn_2(CO)_8L_2]$ (M)
A. L = P(*n*-Bu)$_3$	
9.70×10^2	6.2×10^{-6}
1.45×10^3	1.9×10^{-5}
1.61×10^3	3.7×10^{-5}
1.74×10^3	8.9×10^{-5}
1.75×10^3	1.75×10^{-4}
B. L = P(*i*-Bu)$_3$	
5.65×10^2	3.14×10^{-5}
6.97×10^2	7.85×10^{-5}
8.15×10^2	1.57×10^{-4}

The recombination of CO with the CO-loss species, $Mn_2(CO)_7L_2$*, can be followed in the decay of absorbance in the vicinity of 525 nm. For photolysis under Ar, the decay is comparatively slow and appears to follow second-order kinetics. Generally the bulkier the phosphine ligand, the more stable the semibridged intermediate. At 1 atm of CO, corresponding to [CO] = 1.3×10^{-2} M, the decay is much faster and obeys first-order kinetics. For several solutions at two different concentrations of $Mn_2(CO)_8[P(n\text{-}Bu)_3]_2$, all under 1 atm of CO, the observed first-order rate constant for decay is 77.0 ± 3.0 s^{-1}, which corresponds to a second-order rate constant of 5.7×10^3 M^{-1} s^{-1} (This is in reasonable agreement with the earlier estimate of 9.1×10^3 M^{-1} s^{-1},[3d] when correction is made for a higher assumed concentration of CO in the present work; 0.0135 M[21] vs 0.010 M in the earlier work).

The *a,e*-$Mn_2(CO)_8L_2$ isomer forms as the product of CO reaction with the corresponding semibridged species at low temperature, as demonstrated by IR spectroscopy. It has an absorption peak at around 430 nm, as shown previously and as predictable on the basis of the UV–visible spectra of similar intermediates. The absorbance change at 425 nm upon flash photolysis of solutions of $Mn_2(CO)_8[P(n\text{-}Bu)_3]_2$ under Ar shows a sharp initial decrease, due to bleaching of the starting dimer. This is followed by two steps of recovery, attributed respectively to radical recombinations and reaction of the semibridged intermediate with CO. Apparently no a,e-isomer is formed in substantial amount under these conditions.

When the same experiments are conducted with the solutions under CO instead of Ar, the absorbance *increases* following the flash, due to rapid formation of the a,e-isomer as the result of fast CO recombination. There follows a slower first-order decay, which represents isomerization of the a,e-isomer to the a,a-product. The observed rate constant of about 6 s^{-1} is found for the decay when the ligand is P(*n*-Bu)$_3$. The failure to observe the process under Ar can be readily explained on the basis of the relative rates. The a,e-isomer is first formed via CO recombination with the semibridged intermediate and then isomerizes to the a,a-compound. Under Ar, the bimolecular reaction with CO is so much slower that the following first-order isomerization step does not permit a substantial amount of the a,e-intermediate to accumulate.

Discussion

The technique we have employed, involving flash irradiation at low temperature, with IR detection, permits observation of many intermediate species heretofore not observed. In part the key to success is the use of flash irradiation; continuous irradiation has the potential to excite intermediate species, leading to their rapid conversions to more stable products.

Because so many different species are seen in the $Mn_2(CO)_{10}/PR_3$ or $Mn_2(CO)_8(PR_3)_2$ systems, identification of all of

(20) The numerical simulation was carried out with the HAVCHEM program. The estimated rate constants are 1×10^8 mol^{-1} s^{-1} and 2×10^3 s^{-1}, respectively, for reactions 1 and 2. (See the following references for more detailed description about the program and its application: (a) Stabler, R. N.; Chesick, J. P. *Int. J. Chem. Kinet.* **1978**, *10*, 461. (b) Chesick, J. P. *J. Chem. Educ.* **1988**, *65*, 599. (c) Sullivan, R. J. Ph.D. Dissertation, University of Illinois, Urbana, IL, 1990.)

(21) Cargill, R. W. *Carbon Monoxide*; Solubility Data Series; Pergamon Press: New York, 1990; pp 51–52.

them is difficult. Several lines of argument have proven helpful: (a) Comparisons can be made between these IR band patterns and those of known compounds, e.g., $Mn_2(CO)_8L_2$ compounds previously assigned as e,e-isomers. (b) The appearances of bands seen in irradiation of $Mn_2(CO)_{10}/PR_3$ solutions are consistent with the appearances of those seen in irradiation of the corresponding $Mn_2(CO)_8(PR_3)_2$ solutions. (c) Observations of time-evolution of the spectra at various temperatures show that since intermediates vary greatly in stabilities, some disappear much more readily than others. The complete removal of bands due to one or more intermediates often simplifies the spectra sufficiently to enable identification of the remaining bands. (d) Distinctions between bands resulting from the homolysis path and those due to CO loss can be made by observing the formation of intermediates in frozen glass. Under these conditions, in glasses containing $Mn_2(CO)_{10}$ and PR_3, species derived from substituted radicals are not observed. (e) IR bands due to the semibridging form appear and disappear in concert with the characteristic IR band in the vicinity of 1700 cm^{-1} due to the semibridge species. (f) Concordances of IR spectral changes with the changes in UV–visible spectra help to verify the assignments of the UV–visible bands.

Scheme I summarizes the array of isomers formed and their interconversions following flash irradiation of $Mn_2(CO)_{10}$ and phosphine. Scheme II outlines the species and processes involved following flash irradiation of $Mn_2(CO)_8(PR_3)_2$ solutions. Although, for the axially-substituted derivatives, the eclipsed conformations may be the lowest energy forms, it is likely that, for the equatorially-substituted species, staggered conformations represent energy minima. For ease of visualization, the molecules are shown in the eclipsed conformation closest to the corresponding staggered form. The various formation and isomerization processes are discussed in turn.

***e,e*-$Mn_2(CO)_8[PR_3]_2$ and *a,e*-$Mn_2(CO)_8[PR_3]_2$.** Under the conditions of irradiation employed, employing either xenon flash lamp or 308-nm laser flash irradiation, *both* Mn–Mn bond homolysis and CO loss are expected to be important, for both $Mn_2(CO)_{10}$ and $Mn_2(CO)_8[PR_3]_2$. When diffusive separation of $Mn(CO)_5$ radicals occurs, i.e., at temperatures greater than about 145 K, they undergo rapid substitution by phosphines, yielding $Mn(CO)_4PR_3$. No structural ESR work on the monosubstituted radicals has been reported, but the ESR data for $Mn(CO)_3[PR_3]_2$ radicals indicates that the phosphines occupy basal positions in a square pyramidal structure.[10,22] It is reasonable to expect that the phosphine in $Mn(CO)_4PR_3$ will also occupy a basal position.

The spectral evidence from this work is that the kinetic product of recombination of $Mn(CO)_4L^{\bullet}$ radicals, when L = PMe_3, P(*n*-Bu)$_3$, or P(*i*-Bu)$_3$, is *e,e*-$Mn_2(CO)_8(PR_3)_2$. For P(*i*-Pr)$_3$ and PCy_3, there is no evidence for the e,e-isomer. Rather, the only disubstituted intermediates appear to be the a,e-isomers, although the evidence for them is not as clear-cut as that for *e,e*-$Mn_2(CO)_8[P(n\text{-}Bu)_3]_2$. Presumably the steric requirements of these two ligands preclude formation of the e,e-isomer. Assuming that the axial and basal isomeric forms of the radicals are in equilibrium, with the equilibrium favoring the basal isomer, the following relationships are obtained:

$$b\text{-}Mn(CO)_4L \rightleftarrows a\text{-}Mn(CO)_4L \quad (3)$$

$$2\ b\text{-}Mn(CO)_4L \rightarrow e,e\text{-}Mn_2(CO)_8L_2 \quad (4)$$

$$b\text{-}Mn(CO)_4L + a\text{-}Mn(CO)_4L \rightarrow a,e\text{-}Mn_2(CO)_8L_2 \quad (5)$$

$$2\ a\text{-}Mn(CO)_4L \rightarrow a,a\text{-}Mn_2(CO)_8L_2 \quad (6)$$

For L of moderate size, k_4 is presumably not much smaller than k_5 or k_6. Given that [*b*-$Mn(CO)_4L$] ≫ [*a*-$Mn(CO)_4L$], formation of the e,e-isomer is kinetically favored. For larger L, if $k_4 \ll k_5$, formation of the a,e-isomer is favored.

The kinetics of the isomerization reactions of *e,e*-$Mn_2(CO)_8L_2$ and *a,e*-$Mn_2(CO)_8L_2$ are remarkable, in that the rates are very high in comparison with rates of isomerization at mononuclear six-coordinate metal centers.[23] Isomerization of *e,e*-$Mn_2(CO)_8L_2$

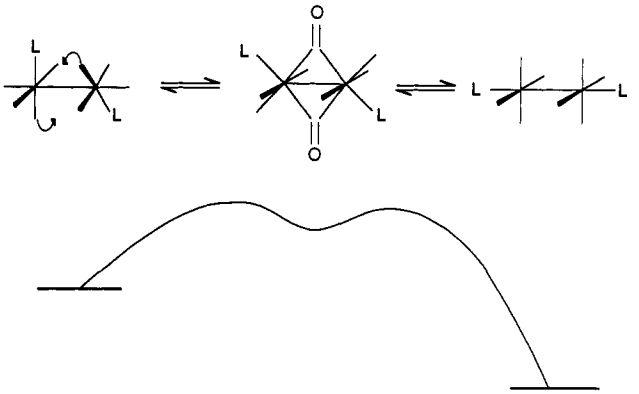

Figure 11. Energy diagram for isomerization of the e,e- to a,a-species through a doubly-bridging CO transient state or intermediate. The e,e-isomer is shown in a staggered conformation.

might occur by one of several pathways:

(a) Thermal Mn–Mn Bond Dissociation. It is known that $Mn(CO)_3L_2^{\bullet}$ radicals, where L = P(*n*-Bu)$_3$ or P(*i*-Bu)$_3$, are persistent.[10] That is, the Mn–Mn bond in $Mn_2(CO)_6L_4$ is weak, presumably because of steric interactions of L with other L or with the CO groups on the other metal. In a $Mn_2(CO)_6L_4$ dimer, two of the L are likely to be in the axial positions, but the remaining two L must be in equatorial locations. It is presumably these L which give rise to the steric repulsions that so weaken the Mn–Mn bond that bond formation is not observed. It is thus reasonable to expect that the Mn–Mn bond should be substantially weakened by the steric interactions of the equatorially placed L groups in *e,e*-$Mn_2(CO)_8L_2$. A facile thermal homolysis of the Mn–Mn bond would lead to formation of the radicals, which could isomerize and, upon recombination, eventually lead to the *a,a*-$Mn_2(CO)_8L_2$ isomer. Such a pathway would be expected to proceed through formation of the intermediate *a,e*-$Mn_2(CO)_8L_2$ isomer. The driving force for the further isomerization of this to *a,a*-$Mn_2(CO)_8L_2$ should be much lower than for the first step, so one would expect a buildup of the a,e-isomer. However, the conversion of the e,e-form is observed to proceed directly to the a,a-form, as shown in Figure 3.

(b) Dissociation of L. If there is sufficient steric pressure in the e,e-isomer, dissociation of L might be facilitated. Rearrangement of the vacated metal center should be facile. Recombination with L could then lead to siting of L in the axial position. Again, however, this mechanism should produce an intermediate a,e-isomeric form.

(c) Intramolecular Rearrangement at the Six-Coordinate Metal Center. While intramolecular rearrangements at six-coordinate metal centers are known,[23] they occur much more slowly than the processes seen here. Further, it is difficult to see how intramolecular processes centered at each metal could be concerted. Thus, such a mechanism should also lead to the intermediacy of an a,e-isomer.

(d) Intramolecular Rearrangement. A concerted intramolecular rearrangement that permits simultaneous movement of the ligands from the equatorial to axial positions would account for our results. We propose that the intramolecular process is one involving formation of bridging CO groups. Although facile formation of bridging CO groups is not established for $Mn_2(CO)_{10}$ or its phosphine-substituted derivatives, pairwise exchange of CO groups has been proposed in $MnRe(CO)_{10}$.[2g] Facile exchange of terminal and doubly-bridged CO is observed for other metal carbonyl compounds of first-row transition elements.[24] Examples include $Co_2(CO)_8$, which exists in bridging and nonbridging forms and

(22) Rattinger, G. B.; Belford, R. L.; Walker, H.; Brown, T. L. *Inorg. Chem.* **1989**, *28*, 1059.

(23) (a) Darensbourg, D. J. In *Advances in Organometallic Chemistry*; Stone, F. G. A., West, R., Eds.; Academic Press: New York, 1982; Vol. 21, p 113. (b) Majunke, W.; Leibfritz, D.; Mack, T.; tom Dieck, H. *Chem. Ber.* **1975**, *108*, 3025. (c) Schenk, W. A. *J. Organomet. Chem.* **1980**, *184*, 1954. (d) Carriedo, G.; Riera, V. *J. Organomet. Chem.* **1990**, *394*, 275.

(24) Evans, J. In *Advances in Organometallic Chemistry*; Stone, F. G. A., West, R., Eds.; Academic Press: New York, 1977; Vol. 16, p 319.

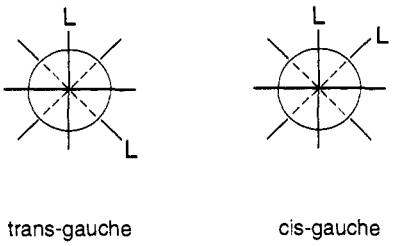

Figure 12. Newman projections of the trans-gauche and cis-gauche conformations of *e,e*-$Mn_2(CO)_8L_2$. The trans-gauche form is probably the lowest energy rotational conformer.

undergoes very facile interconversion between them.[25] Rapid intramolecular exchange of CO groups in $Cp_2Fe_2(CO)_4$ affords another example.[26] Manganese is involved in rapid intramolecular exchange in $[MnFe_2(CO)_{12}]^-$.[27]

A schematic free energy reaction surface for isomerization via formation of bridging CO groups is shown in Figure 11. The lowest energy rotational conformer in *e,e*-$Mn_2(CO)_8L_2$ is likely to be the trans-gauche form, shown in a Newman projection in Figure 12. Formation of a doubly-bridged intermediate could occur via concurrent movement of any pair of CO groups which are roughly trans-gauche to one another. However, only when those which are also trans to the L group on each metal are involved is the intermediate formed that could, upon return to the all-terminal CO structure, shift the L groups into the axial positions. It is particularly significant that the proposed mechanism strongly favors a *concerted* shift of both L from equatorial to axial locations. It thus accounts nicely for the apparent absence of the intermediate a,e-isomer in the process. An a,e-isomer could be formed via a doubly-bridged intermediate, beginning from the cis-gauche conformation of the e,e-isomer. However, this conformation is disfavored on energetic grounds for ligands of significant steric requirement.

The driving force for the e,e → a,a conversion should increase with increasing size of L. Nevertheless, the observed isomerization rate is slightly slower for L = $P(i\text{-}Bu)_3$ than for $P(n\text{-}Bu)_3$. This result suggests that, in the transition state for conversion from the all-terminal to the bridging structure, the environment about the phosphine ligands is more crowded than it is in the ground state.

Although the a,e-isomer is not formed as an intermediate in the e,e → a,a isomerization, it is produced upon reaction of CO with the semibridging species. A point of importance is that the a,e → a,a conversion is substantially slower for a given L than the e,e → a,a conversion. This might be expected on general grounds, inasmuch as the driving force for the process is much lower. The observation that the a,e → a,a conversion is so much slower, however, is further evidence that the a,e-isomer is not an intermediate in the e,e → a,a conversion. If it were, its concentration would have built up during the process.

A schematic diagram representing isomerization of the a,e-form is shown as Scheme III. Assuming that the process occurs via formation of CO bridges, as before, one immediate conclusion is that there is no single step which can convert the a,e-isomer to the a,a-isomer. Inevitably, any process that moves the equatorially-located L into an axial position simultaneously interconverts the axially-located L to an equatorial position (Scheme IIIa). The isomerization is thus a two-step process, in which the a,e-isomer is first converted to the e,e-form (Scheme IIIb). Further, the e,e-isomer which is formed initially is one in which the L groups are in a more or less cis-gauche conformation. There follows a rotation about the Mn–Mn bond to yield the lower energy trans-gauche e,e-isomer, and then the single-step conversion of the e,e-isomer to the a,a-isomer occurs, as shown in Figure 11.

(25) (a) Noack, K. *Spectrochim. Acta* **1963**, *19*, 1925; *Helv. Chim. Acta* **1964**, *47*, 1064. (b) Bor, G.; Noack, K. *J. Organomet. Chem.* **1974**, *64*, 367. (c) Sweany, R.; Brown, T. L. *Inorg. Chem.* **1977**, *16*, 415.
(26) Adams, R. D.; Cotton, F. A. *J. Am. Chem. Soc.* **1973**, *95*, 6589.
(27) Forster, A.; Johnson, B. F. G.; Lewis, J.; Matheson, T. W.; Robinson, B. H.; Jackson, W. G. *J. Chem. Soc., Chem. Commun.* **1974**, 1042.

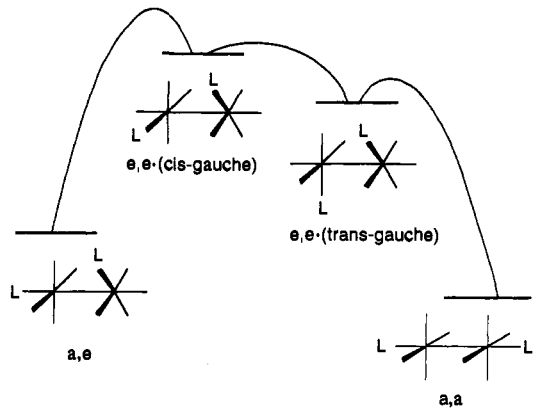

Figure 13. Energy diagram of the isomerization of the a,e- to a,a-form. The process proceeds through an e,e-(cis-gauche)-isomer as an intermediate. The rotational isomers of molecules with equatorially-located L are shown as staggered conformations.

Scheme III

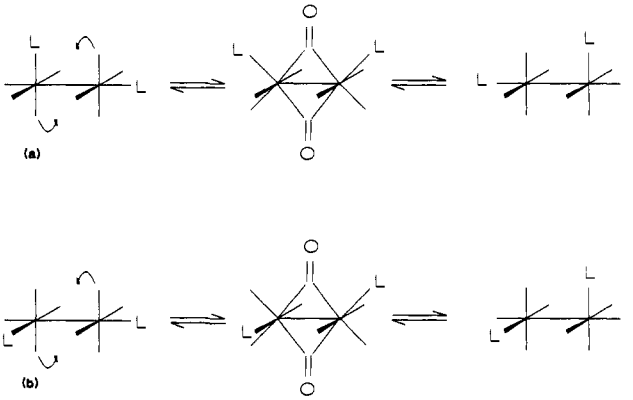

The intermediacy of the cis-gauche isomer explains in part why the e,e-isomer converts less readily to the a,e-isomer than to the a,a-isomer. The other contributory factor is that if the intrinsic barriers for formation of the doubly-bridged form were the same, the more exergonic process would have the lower free energy barrier.

The role of a rotational motion in determining the relative rates of two isomerization processes in the present system is roughly analogous to the role of rotation in determining the relative rates of bridge-terminal exchange in *cis*- and *trans*-$Cp_2Fe_2(CO)_4$.[26] A schematic free energy diagram for the overall process is shown in Figure 13. We can assume that the e,e-isomer lies significantly above the a,a-isomer in energy; the energy of the a,e-isomer is likely to lie between the values for the e,e- and a,a-isomers. We do not know how the barriers to isomerization depend on the details of the locations of the ligands nor even whether the bridging CO forms are transition states or intermediates. However, the scheme accounts reasonably well for the observed relative rates. The rate of a,e → a,a conversion for $Mn_2(CO)_8(P(n\text{-}Bu)_3)_2$ is about 250-times slower at room temperature than that of the e,e → a,a conversion; this corresponds to a difference in free energies of activation of about 3.3 kcal mol^{-1}. From the fact that there appears to be about a 1% population of the a,e-isomer in equilibrium with the a,a-isomer at room temperature, we can infer that the molar free energy of *a,e*-$Mn_2(CO)_8[P(n\text{-}Bu)_3]_2$ is about 2.7 kcal mol^{-1} higher than that of *a,a*-$Mn_2(CO)_8[P(n\text{-}Bu)_3]_2$. If the intrinsic barriers to formation of the bridging forms were about the same for the a,e- and e,e-isomers, the difference in free energies of activation would be consistent with a free energy difference of about 3.5 kcal mol^{-1} between the a,e- and e,e-isomers. Thus, the e,e-isomer is estimated to be about 6 kcal mol^{-1} higher in energy than the a,a-isomer.

$Mn_2(CO)_7L_2$*. Photochemical loss of CO from $Mn_2(CO)_{10}$ leads initially to formation of a solvent-coordinated species,

$Mn_2(CO)_9(S)$. The solvent molecule (S) is very rapidly replaced by a CO from the adjacent metal center, forming the semibridging form, $Mn_2(CO)_8(\eta^1,\eta^2\text{-CO})$, denoted $Mn_2(CO)_9$*. The flash experiments carried out at 90 K reveal an intermediate that decays in about 30 min, forming $Mn_2(CO)_9$*. The IR bands of the intermediate are consistent with its formulation as the solvent-coordinated species.

For L = P(*n*-Bu)$_3$, the species initially formed at 173 K exhibits an IR band assignable to the semibridging CO, at 1701 cm^{-1}. However, this species decays to form two other species with IR bands at 1715 and 1687 cm^{-1}. We propose that the initially-formed species is the a,a-semibridged form, as shown in Scheme II. Exchange of the semibridging CO group between the two metals in $Mn_2(CO)_5$[dppm]$_2$, which possesses a well-characterized semibridging CO group, has been shown to be slow on the ^{31}P NMR time scale at room temperature.[9f] Lacking any evidence to the contrary, we assume that the only kinetically significant mode of CO rearrangement in $Mn_2(CO)_7L_2$* at 173 K is the opening and closing of the semibridge and associated rearrangements at the open metal center. Rate constants of 550 and 250 s^{-1} at room temperature have been estimated for opening of the semibridge in $Mn_2(CO)_7$[P(*n*-Bu)$_3$]$_2$* and $Mn_2(CO)_7$(PMe$_3$)$_2$*, respectively.[7d] Thus, the "bridge off" process might well occur in the time regime of 10–100 min at 173 K.

We have discussed elsewhere[7d] the evidence for a significant barrier to re-formation of the semibridge from the open form, beyond that due to dissociation of any solvent molecule that may occupy the otherwise vacant site at the metal. With the metal center either momentarily vacant or weakly coordinated by solvent, rearrangement at the center should be facile, thus providing a pathway for movement of L from one site to another. As shown in Scheme II, the appearance of two new characteristic frequencies for the semibridging CO could be accounted for in terms of the siting of L in either of two equatorial sites. While the ligand is not located preferentially in the equatorial site in the fully coordinated form, it could be sited preferentially in an equatorial location in the semibridged species. Admittedly, the frequencies of the semibridging CO group form a slim basis for assignments of the structures of the isomers. However, the conjecture that isomerization occurs at the site at which the semibridging CO is coordinated in η^2 fashion seems the most reasonable alternative at this time.

Upon loss of CO from $Mn_2(CO)_8$[PMe$_3$]$_2$, the semibridging species formed exhibits an IR band at 1717 cm^{-1}, consistent with our hypothesis that an equatorially-located phosphine gives rise to a band at 1715 cm^{-1} in the case of L = P(*n*-Bu)$_3$. There is also weak evidence for a second band at 1692 cm^{-1}, which could correspond to a PMe$_3$ ligand in the second of two alternative equatorial locations, as shown in Scheme II. Presumably the PMe$_3$ ligand bound to the metal containing the η^1 coordinated CO is in an equatorial position as well. In this regard, the results for $Mn_2(CO)_{10}(PMe_3)_2$ support the hypotheses regarding the isomerizations operating in $Mn_2(CO)_7$[P(*n*-Bu)$_3$]$_2$. However, the one puzzling result is that upon addition of CO the *a,e*-$Mn_2(CO)_8$[PMe$_3$]$_2$ isomer is formed, whereas one would expect the e,e-isomer. At this point we have no convincing explanation for this apparent anomaly.

Finally, it should be noted that the observed rate of reaction of CO with $Mn_2(CO)_7$[P(*n*-Bu)$_3$]$_2$* is consistent with the rate for this process measured earlier.[3d] A detailed account of the kinetics of reaction of $Mn_2(CO)_9$* with CO and other ligands will be reported elsewhere.

***e*-$Mn_2(CO)_9L$.** Reaction of $Mn_2(CO)_9$* with P(*n*-Bu)$_3$ following flash photolysis of solutions containing $Mn_2(CO)_{10}$ and P(*n*-Bu)$_3$ at 143 K occurs over a period of 1 or 2 min, and yields *e*-$Mn_2(CO)_9$P(*n*-Bu)$_3$ as initial product. This isomer converts to the thermodynamically more stable *a*-$Mn_2(CO)_9$P(*n*-Bu)$_3$ with a rate constant at 297 K of 12 s^{-1}. It is interesting that this rate constant is substantially smaller than that for the process *e,e*-$Mn_2(CO)_8$[P(*n*-Bu)$_3$]$_2$ → *a,a*-$Mn_2(CO)_8$[P(*n*-Bu)$_3$]$_2$. The thermodynamic driving force should be smaller for isomerization of the monosubstituted compound. At the same time, if the isomerization process involves formation of a doubly-bridging CO intermediate, as seems reasonable, the intrinsic barrier for the process should be comparable to that for isomerization of the disubstituted compound. In this event, the free energy barrier will be higher for the less exergonic process, i.e., for isomerization of the monosubstituted compound, as observed.

In summary, the use of a combination of flash irradiation coupled with low-temperature IR detection and room-temperature UV–visible transient spectroscopy has revealed a rich assortment of previously unknown geometric isomer formations and isomerization processes. Similar intermediates and their corresponding isomerization processes are likely to exist in both the photochemical and thermal reactions of other dinuclear carbonyl systems, and possibly in carbonyl clusters as well. The steric requirements of the substituting ligands and metal–metal bond distances are probably the most critical factors determining the kinetic and the thermodynamic properties of the intermediates. From these studies it is clear that the manganese dinuclear carbonyl system passes through several stages in the overall process of reaching the thermodynamically stable state. During the lifetimes of the various intermediates, chemical processes not accessible to the ground-state molecule might occur. Thus, it is important that such intermediates and their time dependencies be known if we are to fully understand the photochemical reactivities of the system toward a variety of substrates.

Acknowledgment. This research was supported by the National Science Foundation through Grant CHE89-12773. The authors are grateful to Dr. Shulin Zhang for assistance and helpful discussions.

Supplementary Material Available: Figures showing (a) difference IR spectra for $Mn_2(CO)_{10}$ and P(*n*-Bu)$_3$ in 3-methylpentane at 243 K following a single flash; (b) difference IR spectra for $Mn_2(CO)_8$[P(*n*-Bu)$_3$]$_2$ in 3-methylpentane at 173 K following a single flash; and (c) analogous difference spectra for $Mn_2(CO)_8$[P(*n*-Bu)$_3$]$_2$ at 243 K (4 pages). Ordering information is given on any current masthead page.